

CONF 861207-82  
006971  
MAR 25 1987

LASER PHOTOACOUSTIC SPECTROSCOPY FOR TRACE LEVEL  
DETECTION OF ACTINIDES IN GROUNDWATER

MARK M. DOXTADER,\* VICTOR A. MARONI,\* JAMES V. BEITZ,\* AND  
MICHAEL HEAVEN\*\*

\* Argonne National Laboratory, 9700 South Cass Avenue, Argonne, IL 60439

\*\* Department of Chemistry, Illinois Institute of Technology, Chicago,  
IL 60616

CONF-861207--82

DE87 006971

## INTRODUCTION

The Basalt Waste Isolation Project (Rockwell Hanford Operations-BWIP) is investigating the feasibility of building a repository in the Columbia River Basalts for the permanent disposal of high-level nuclear waste. One aspect of this effort is to develop an understanding of the chemical behavior of radionuclides in the near-field environment of the waste container. Such information is needed to determine radionuclide release rates from the waste package and to make long-term projections of repository performance. To accomplish this task, ultrasensitive laser-based techniques, such as laser photoacoustic spectroscopy (LPAS) and laser induced fluorescence (LIF), are being developed as analytical methods for the trace-level detection and speciation of actinides in solutions typical of those encountered in groundwaters near the BWIP repository.

These sensitive spectroscopic methods are being developed because initial characterization of the repository environment has suggested that those actinide elements of greatest interest to long-term repository performance, Pu and Am, will be quite insoluble in the BWIP groundwater. These techniques will provide the most refined data possible to be used as input for development and validation of the codes that will be used to describe and project repository performance. The most useful application of the techniques will be when applied directly to conditions anticipated to exist in the repository after containment failure. Such conditions include repository groundwater at elevated temperature, in contact with waste package components. Studies done using in situ conditions will allow the qualitative aspects of actinide complexation to be examined as a function of the redox state of the system, and will provide data to support steady-state solubility studies being done in other parts of the BWIP program.

In this paper we examine the utility of the LPAS technique for elucidating the chemical behavior of species present in the near-field environment of the BWIP repository. We briefly review the existing basis for interpreting actinide spectra at low concentrations, and describe our initial experiments. These experiments include development and demonstration of the methodology under optimum conditions, e.g., stable, well-characterized solutions of holmium; and application of the technique to conditions relevant to the repository, including studies performed with uranium in synthetic groundwater and at elevated temperatures.

## BACKGROUND

Optical absorption spectroscopy can be used to characterize actinide complexes in solution because the "fingerprint" nature of the observed f-f transitions allows identification of the element and oxidation state in favorable cases. Spectra of most of the known oxidation states of actinide ions, generally in favorable acid solutions or solid phases, have

The submitted manuscript has been authored by a contractor of the U. S. Government under contract No. W-31-109-ENG-38. Accordingly, the U. S. Government retains a nonexclusive, royalty-free license to publish or reproduce the published form of this contribution, or allow others to do so, for U. S. Government purposes.

## **DISCLAIMER**

This report was prepared as an account of work sponsored by an agency of the United States Government. Neither the United States Government nor any agency thereof, nor any of their employees, makes any warranty, express or implied, or assumes any legal liability or responsibility for the accuracy, completeness, or usefulness of any information, apparatus, product, or process disclosed, or represents that its use would not infringe privately owned rights. Reference herein to any specific commercial product, process, or service by trade name, trademark, manufacturer, or otherwise does not necessarily constitute or imply its endorsement, recommendation, or favoring by the United States Government or any agency thereof. The views and opinions of authors expressed herein do not necessarily state or reflect those of the United States Government or any agency thereof.

been reviewed by Carnall [1] and more recently, Carnall and Crosswhite [2]. From these studies it is evident that, while unique, such transitions are weak, making conventional absorption spectrometers, which rely on pronounced differences in light absorption, too insensitive for trace-level detection of actinides. Recently, LPAS [3] has been utilized for oxidation-state-specific detection and speciation of actinides in aqueous solution. Using this technique, detection limits of  $10^{-6}$  to  $10^{-8}$ M were obtained for several actinides in acid media [4,5].

The conditions of interest to BWIP, e.g., elevated temperature, groundwater, equilibration with waste package components (mineral phases and carbon steel) are not those that have been routinely pursued by groups studying actinide chemistry. However, information and established descriptions of actinide speciation that have been collected under specialized conditions in order to aid data interpretation, will be useful in guiding the development of the present experimental setup and in interpretation of what likely will be complex spectra.

For example, groundwater samples are different from simple solutions because they will contain a variety of metal ions and complexing ligands. Basalt groundwater of interest to the BWIP effort (see Table I) contains carbonate, sulfate, fluoride, and other anions which are capable of complexing actinide ions. Since both the electronic structure and the transition intensities of actinide ions are influenced by ligand field effects, care will have to be exercised when applying the acid solution and solid literature to the interpretation of spectra collected in groundwater. However, it is expected that complexed actinides in near neutral pH solutions will exhibit "fingerprint" spectra involving 5f electronic states, and that by selective modification of the groundwater chemistry it may be possible to develop a working theory to describe the character of spectra under varying repository conditions.

While optical absorption spectra of actinides in near-neutral pH solutions containing a variety of complexing ligands (GR-4 groundwater) have not been extensively explored, we have found a significant body of data pertaining to actinide carbonate complexes that provide a useful starting point for our present study. Newton and Sullivan [6] recently reviewed literature concerning actinide carbonate complexes including spectroscopic studies.

TABLE I

Composition of Synthetic Grande Ronde #4  
(GR-4) Solutions<sup>9</sup> at pH 9.7

Chemical Species	Concentration (mg/L)
Na	334
K	13.8
Ca	2.2
F	19.9
Cl	405
SO <sub>4</sub>	4.0
Inorganic Carbon	18.1
Si	45.0

Electronic spectra of actinide carbonate complexes have usually been reported for rather high concentrations of bicarbonate and/or carbonate (typically 0.1M). Such concentrations favor the formation of complexes containing two or more carbonates per actinide ion. Basalt groundwater of interest to the BWIP effort typically contains about 0.0011M bicarbonate and 0.0004M carbonate. The literature spectra will be helpful in interpreting spectra collected in the BWIP groundwater if the same complexes are present throughout the range of carbonate concentrations studied.

Additional optical spectra of complexed transuranic ions at sub-micromolar concentrations at near-neutral pH have been reported by Kim and co-workers [5]. They report the LPAS spectrum for 0.5 micromolar  $\text{Am}^{+3}$  in 0.1M sodium carbonate solution at pH 6.7, but do not provide any evidence or speculation concerning the complexed species which contribute to the observed spectrum. In a later report [7] it is suggested that three  $\text{Am}(\text{III})$  species are present, a monocarbonatodihydroxo, a monohydroxodicarbonato, and a hydroxo complex. This emphasizes the need to consider mixed ligand complexes in the case of basalt groundwater, and suggests the possibility of using a range of groundwater concentrations to characterize species of interest.

The nature of the species formed will also likely depend on other parameters, including temperature. Maximum temperatures on the order of 150°C are anticipated during the isolation period. Oxidation state distributions, stability, and solubility constants are temperature dependent, and the temperature dependence of each of these factors will need to be incorporated into models describing repository performance. To date, little thermodynamic solution data concerning actinides at temperatures above 25°C are available, and common methods used to extrapolate these data to higher temperatures [8] do not take into account the potential changes in complexation that may occur as the temperature is increased. This accentuates the importance in collecting spectra in conditions that are repository relevant.

## EXPERIMENTAL

A schematic of the experimental arrangement is shown in Figure 1. The excitation source consisted of a dye laser (Moletron DL16) pumped by the third harmonic of a  $\text{Nd}^{+3}/\text{YAG}$  laser (Quanta-Ray DCR-2A). This system was operated at a maximum energy of 3 mJ at 10 Hz, as monitored by two energy monitors located downfield from the sample cells. The bandwidth of the laser was  $<1 \text{ cm}^{-1}$  and its pulse width was  $\sim 5 \text{ ns}$ .

The output of the laser was directed into the sample compartments of a single beam, dual transducer, photoacoustic spectrometer (see Figure 2). This arrangement allowed real-time subtraction of the photoacoustic signal due to optical absorbance of water. The blank (GR-4 water or 0.1M  $\text{HClO}_4$ ) and sample solutions, contained in 1 x 1 cm quartz cuvettes, were housed in aluminum blocks capable of heating the solutions to temperatures in excess of 80°C. For work above ambient temperature the cells were sealed under partial vacuum. To prevent condensation onto the upper surfaces, the portion of the sealed cell above the liquid/air interface was maintained at a temperature slightly greater than the solution. Acoustic contact to the cell was achieved by means of a 1 cm diameter x 10 cm long quartz rod which in turn was in contact with a silvered mirror. Contact with a piezoelectric transducer (PZT) (Transducer Products LTZ-2, 9 mm diameter, 5 mm thick) was made through a thin, stainless steel membrane that was part of the housing which was in contact with the mirror. This combination eliminated problems associated with scattered light with  $\sim 40\%$  loss in acoustic signal while isolating the transducer from the adverse effects of elevated temperature. To improve acoustic contact, a thin layer of chloro-fluorocarbon grease was applied to all appropriate surfaces.

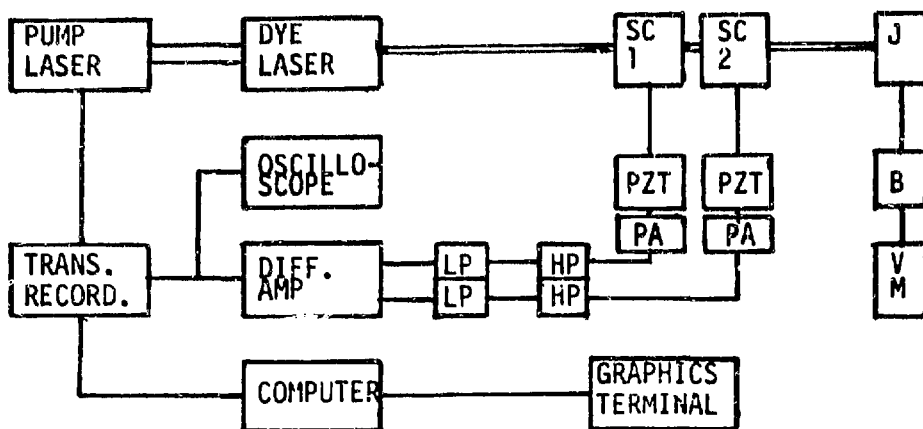


Figure 1. Block diagram of the single beam, dual channel laser photoacoustic spectrometer. The major components are as follows:

COMPUTER -	Digital Equipment Corporation 11/23+.
DIFFERENTIAL AMPLIFIER -	Tektronix AM502.
VM -	Digital voltmeter.
DYE LASER -	Molelectron DL16 dye laser with home-built post amplifier. Typical output energy was a 3 mJ/pulse in a 5 ns pulse.
HP -	High pass electrical filter, 10th order design, passive components.
J -	Molelectron Joulemeter.
LP -	Low pass electrical filter, 1st order design, passive components.
PRE-AMP (PA) -	Analog Devices 50K operational amplifier in a custom designed, variable gain, circuit.
PUMP LASER -	Quanta Ray DCR-2A operated at 355 nm at 10 Hz rep. rate
PZT -	9 mm dia. by 5 mm thick solid cylinder piezoelectric transducer (LTZ-5A material) in stainless steel housing.
SC -	Sample cell, 1 x 1 cm i.d., quartz, polished five sides.
TRANSIENT RECORDER -	LeCroy TR8818 (10 ns per channel best time resolution).
B -	Brookdeal linear gate

The signals were preamplified using operational amplifiers with FET inputs (Analog Devices 50K). Use of variable gain operational amplifiers facilitated individual balancing of the two PZT signals. Amplified signals were filtered by low and high pass filters to eliminate unwanted frequency components present in the waveform and then coupled to the inputs of a differential amplifier (Tektronix AM502). The output of the differential amplifier [(analyte + solvent) - (solvent)] was digitized by a transient recorder (LeCroy TR 8818) and signal averaged on a computer (Digital 11/23+) for further analysis.

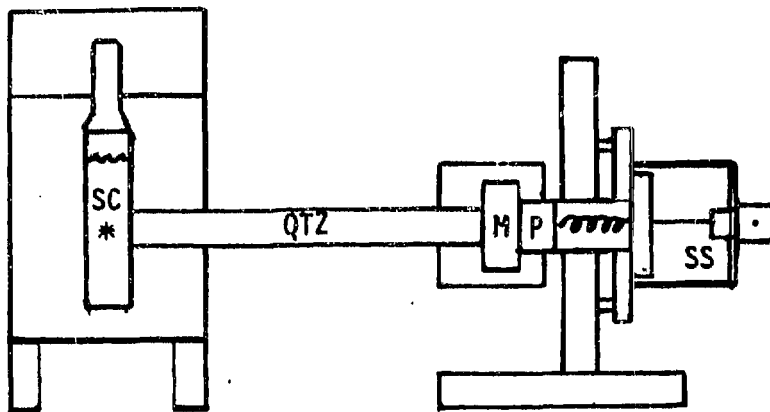


Figure 2. Cross section view of a single sample cell block showing relative positions of sample cell, quartz rod, silver mirror and stainless steel piezoelectric transducer housing.

- M - 2.54 cm diameter, 0.63 cm thick, front surface, silvered dielectrically coated, borosilicate substrate.
- PZT - 0.9 cm diameter, 0.5 cm thick piezoelectric transducer.
- QTZ - 1.0 cm diameter, 10 cm long, fused quartz rod.
- SC - 1.000 x 1.000 cm quartz sample cell, flame sealed.
- SS - Stainless steel housing

Synthetic groundwater (GR-4 water) was prepared in accordance with the procedures stipulated by the BWIP program [9]. Stock solutions of uranyl perchlorate were prepared from  $U_3O_8$  (NBS 950a certified). An aliquot of this solution was taken to dryness and redissolved in GR-4 water. Small adjustments in the pH of the resulting solution were made using dilute NaOH to obtain a final value of 9.7. Further dilutions were made to achieve final uranyl perchlorate concentrations between  $10^{-4}$  and  $10^{-6}$  M. Sensitivity measurements of the spectrometer were made by using holmium (III) perchlorate in 0.1 M perchloric acid. All solutions were filtered into the cuvettes prior to analysis using 0.45 micron filters (Gelman Acrodisc-CR).

The actual operating procedures required an initial balancing of the acoustic waveforms from the sample and reference channels. With the solvent (i.e., GR-4 or 0.1 M perchloric acid) in both cells, adjustments in phase and amplitude were made by lateral translation of the cell compartments and by varying the gain of the amplifiers. Difference waveforms (solvent vs. solvent) were then recorded for each wavelength of interest. Afterwards, the solvent in the sample cell was removed and replaced with the solution containing the analyte. Again the difference between the reference and sample channels was recorded as a function of those wavelengths measured previously. At each wavelength several signal averaging runs were made, each involving as many as 1024 shots. During the course of the experiment the laser energy was monitored by means of two independent energy monitors. Excitation spectra were obtained by plotting the normalized photoacoustic signal vs. wavelength. At each wavelength, any mean residual difference photoacoustic signal resulting from the neat solvent vs. neat solvent runs was subtracted from the mean difference photoacoustic signal resulting from the solution of interest vs. neat solvent runs. This procedure was adopted to correct for small variations in sample vs. reference channel imbalance as a function of laser wavelength. Dilution curves were obtained in a similar manner by plotting the resultant signal for a specified wavelength as a function of concentration.

## RESULTS AND DISCUSSION

### Sensitivity

Preliminary experiments were performed to determine the overall sensitivity of the apparatus in two different ways. The first evaluation was based on signal-to-noise ratio measurements using a single PZT transducer in direct contact with the sample cell and a solute with an absorption band that was narrow compared to the rate of change of the absorbance of water [3]. The solute that was selected was holmium perchlorate present at a concentration of 0.00487 M in perchloric acid. The molar absorptivity of the 450.7 nm band of Ho(III) is  $3.90 \text{ M}^{-1} \text{ cm}^{-1}$ . Based on repeated signal averaging runs, the signal-to-noise ratio achieved with this solution was 700, averaging over 100 laser shots. This corresponds to a detection sensitivity (signal-to-noise of 1) of about  $2.8 \times 10^{-5}$  absorbance units (a.u.) per cm [10] of optical path through the sample solution. These results were confirmed by eliminating the contribution of water absorption in the excitation spectrum of  $2 \times 10^{-4}$  Ho(III) in the region covering 460-500 nm using the differential mode of operation (see Figure 3). The peak at 486 nm has a molar extinction coefficient of  $1.89 \text{ M}^{-1} \text{ cm}^{-1}$ . Averaging 100 laser shots for each resolution element, a signal-to-noise ratio of 15 was obtained. Thus, for a signal-to-noise of 1 the limit of detection is  $2 \times 10^{-5}$  a.u. per cm of path length.

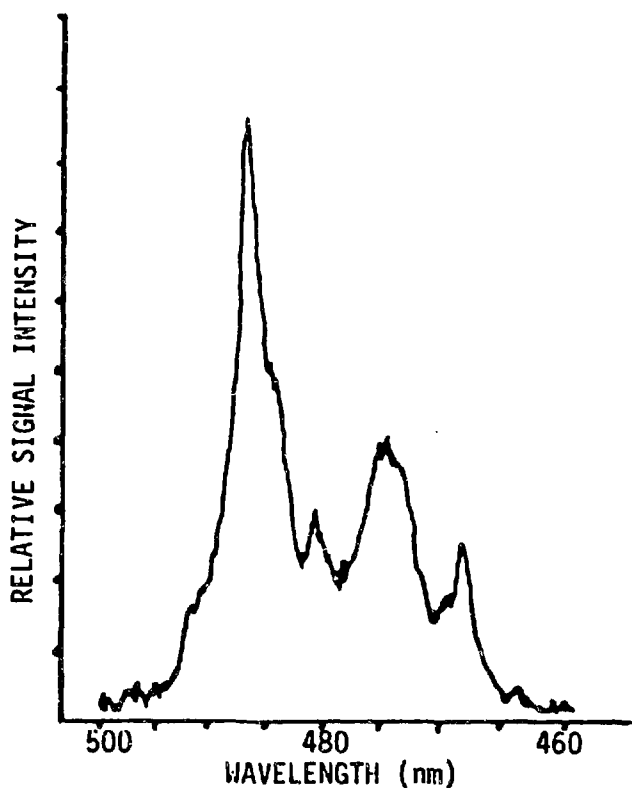


Figure 3. Differential photoacoustic spectrum of  $2 \times 10^{-4}$  M  $\text{Ho}^{3+}$  in dilute  $\text{HClO}_4$ . Spectrum not corrected for dye laser intensity.

Sensitivity measurements is based on measured dilution curves using the difference photoacoustic signal between sample (analyte and solvent) and reference channels (neat solvent). For this study we had selected uranyl ion in 0.1 M perchloric acid due to the extensive spectroscopic studies of Bell and Biggers [11]. Using 427 nm excitation, and interpolating between data points on the dilution curve, a signal-to-noise of 1 occurs at  $7 \times 10^{-6}$  M uranyl (see Figure 4). The molar absorptivity of uranyl at 427 nm is  $5.9 \text{ M}^{-1} \text{ cm}^{-1}$ . Thus, the sensitivity of the laser photoacoustic spectrometer used in the differential mode is equivalent to an absorbance of  $4 \times 10^{-5}$  a.u. This is the sensitivity reported by Schrepp and co-workers [4].

Dilution curves were also constructed for uranyl in GR-4 water (see Figure 5). In repeated measurements, deviations from linearity were observed at concentrations approaching  $10^{-5}$  M. Such deviations may represent significant changes in equilibria at these concentrations. Preliminary measurements using laser induced fluorescence support the existence of more than one uranyl species. The larger range of values for GR-4 vs. GR-4 measurements noted in the caption of Figure 5 is attributed to long-term fluctuations in the laser beam path through the photoacoustic cells.

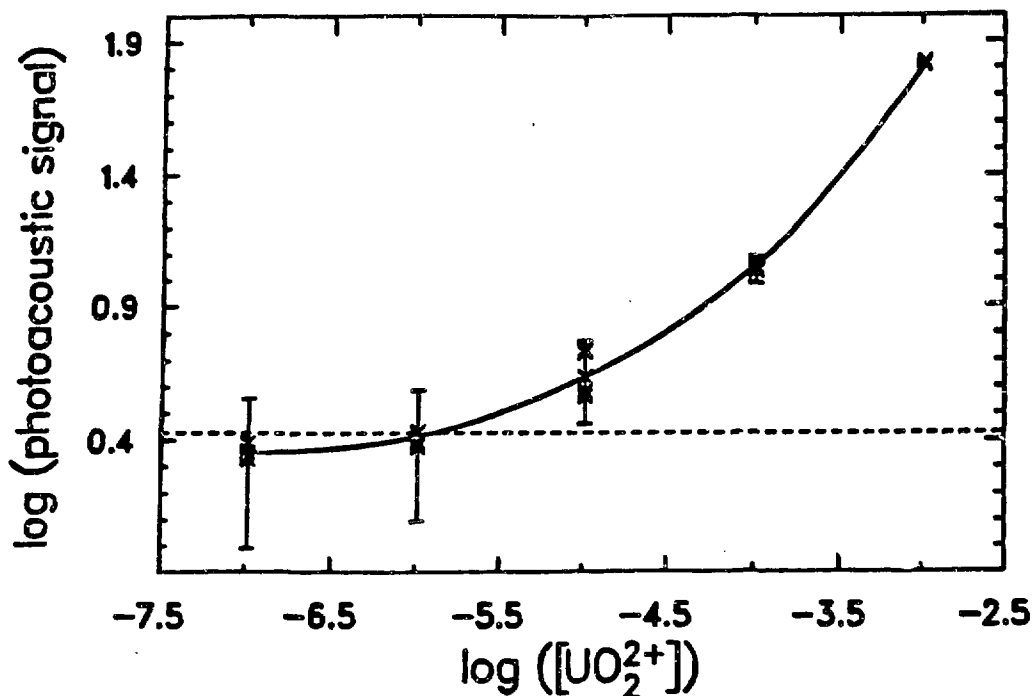


Figure 4. Dilution curve for uranyl ion ( $\text{UO}_2^{2+}$ ) in 0.1 M perchloric acid at 22°C. Uranyl concentrations are in moles/liter. The error bars shown correspond to 2 standard deviations based on replicate determinations. The experimental points are shown as X's. The major source of uncertainty lies in the range of values found when running 0.1 M perchloric acid vs. 0.1 M perchloric acid. A constant value has been added to each data point so that negative values could be plotted on a log axis. The solid line is a smooth curve interpolation between the mean values for each of the 5 uranyl concentrations run. The horizontal dashed line corresponds to the mean value of the 0.1 M perchloric acid vs. 0.1 M perchloric acid runs.



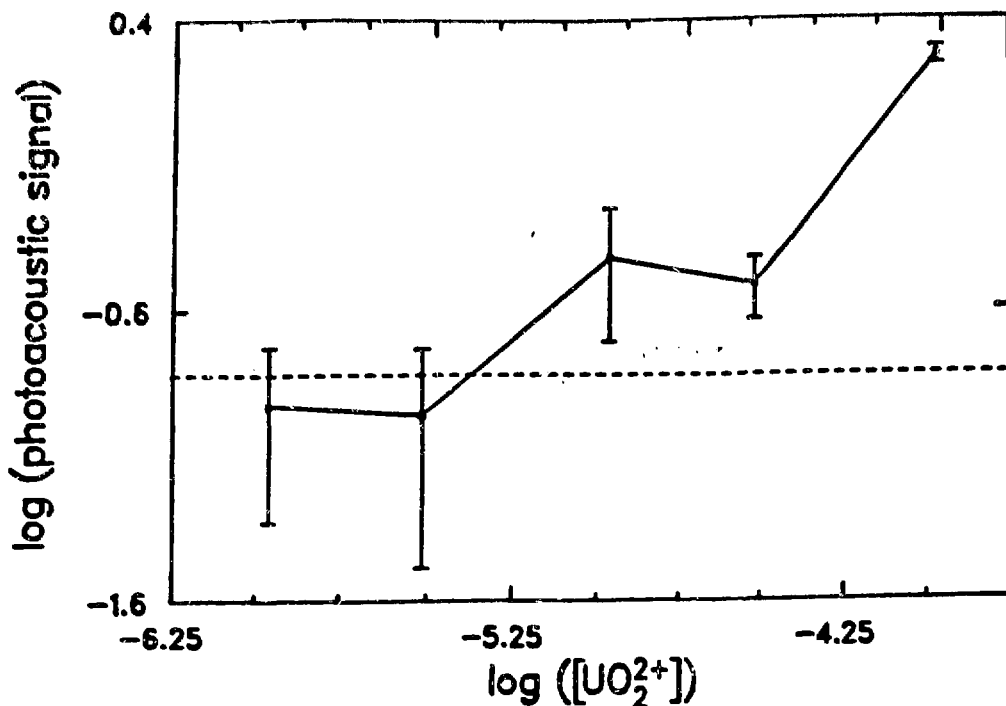


Figure 5. Dilution curve for uranyl ion ( $\text{UO}_2^{2+}$ ) in GR-4 water (synthetic groundwater) at  $22^\circ\text{C}$ . Uranyl concentrations are in moles/liter. The error bars shown correspond to two standard deviations based on replicate determinations. The major source of uncertainty lies in the range of values when running GR-4 water vs. GR-4 water. A constant value has been added to each data point so that negative values could be plotted on a log axis. The solid line has been shown drawn between the mean values for each of the 5 uranyl concentrations. The horizontal dashed line is the mean value of the GR-4 vs. GR-4 water runs.

Photoacoustic spectroscopy at longer wavelengths will be limited by the absorbance of water itself unless the effect of this interference can be eliminated. The ability of the single beam, dual transducer spectrometer to minimize the effect of solvent absorbance more than compensates for the small loss in absorbance sensitivity due to the increased noise incurred in using two transducers.

### Photoacoustic Spectra

Figure 6 shows the observed photoacoustic spectrum from  $1.1 \times 10^{-4}$  M uranyl in GR-4 water at  $22^\circ\text{C}$ . Data were collected at every even nanometer from 420 to 460 nm (+ points) and then at every odd nanometer in this same region (x points). The peak to peak deviation of 15% represents long term fluctuations in overall sensitivity of the apparatus. The solid line is the result of averaging adjacent points.

Figure 7 shows the spectrum observed for the same solution at  $76^\circ\text{C}$ . Data was collected in a similar fashion to that described above. The error limits correspond to the 90% confidence interval and so represent a significant improvement in the stability of the system. This increase in stability results from the use of sealed cells, the reduction of particulate matter, and methods utilized to remove scattered light (e.g., quartz rod and silvered mirror). It is important to note that due to the nature

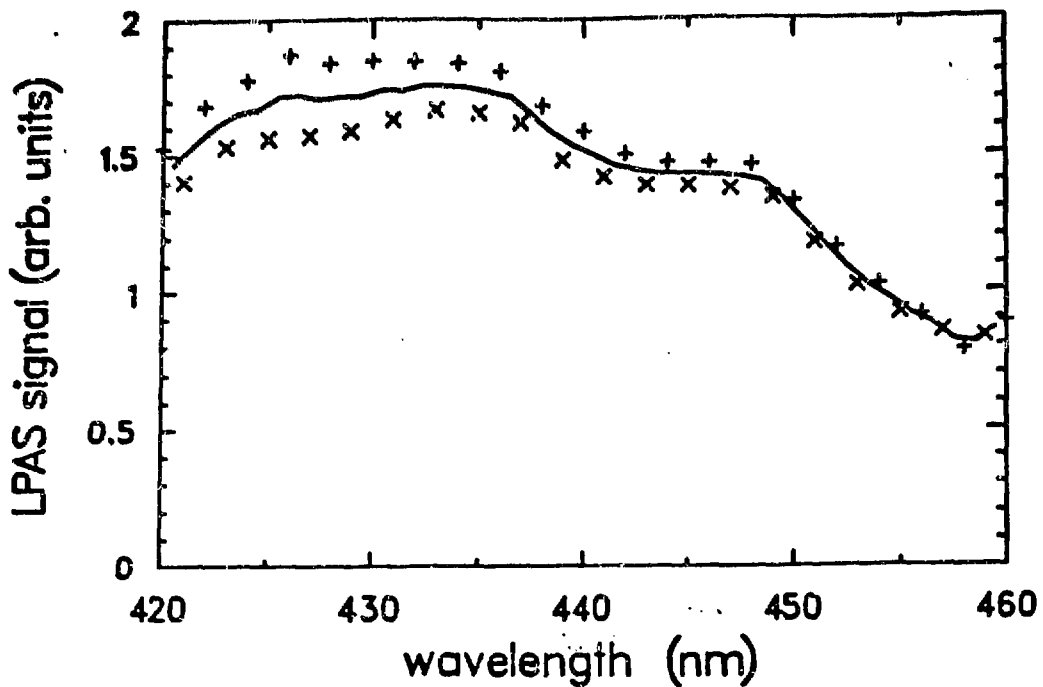


Figure 6. Photoacoustic spectrum observed from  $1.1 \times 10^{-4}$  M uranyl ( $\text{UO}_2^{2+}$ ) in GR-4 water (synthetic basalt groundwater) at  $22^\circ\text{C}$ . The effective wavelength resolution is 2 nm. The scatter in the data points results from slow drifts in the spectrometer sensitivity due in part, to the settling of suspended particulate matter.

of the detection method, signals were actually enhanced at elevated temperatures. Based on theories concerning photoacoustic wave generation [3], the ratio of the peak photoacoustic signal from pure water at  $76^\circ\text{C}$  to that at  $22^\circ\text{C}$  is expected to be 2.71, if the optical absorbance of water is independent of temperature. The measured ratio at 435 nm for GR-4 water at  $76^\circ\text{C}$  and  $22^\circ\text{C}$  is 4.04. This larger value is presumably due to an increase in the optical absorbance of GR-4 water at 435 nm with increasing temperature.

The spectra shown in Figures 6 and 7 are not readily interpretable as arising from dicarbonato and tricarbonato uranyl species. In Figure 3 we plot the expected spectra for a variety of ratios of tris carbonato uranyl to dicarbonato uranyl, based on the reported absorption spectrum of these species given by Scanlan [12]. The LPAS spectra at  $22^\circ\text{C}$  and  $76^\circ\text{C}$  contain significantly less structure than would be expected for tricarbonato uranyl, dicarbonato uranyl or a mixture of these two species. Based on the amount of carbonate and bicarbonate in the GR-4 water, the uranyl would be expected to be present as the tricarbonato species only. However, this conclusion rests on the assumption that uranyl is not present as a colloid and is not complexed by any other species present in the GR-4 water. In fact the rather featureless LPAS spectra combined with the smaller absorptivity of the uranyl in GR-4 solutions suggest that the uranium is present as a multinuclear complex and that one or more hydroxo ligands may be associated with each uranyl.

At this time we do not anticipate experimental difficulties due to scattered laser light in the measurement of low density colloids via photoacoustic spectroscopy. Interpretation of such data, however, will

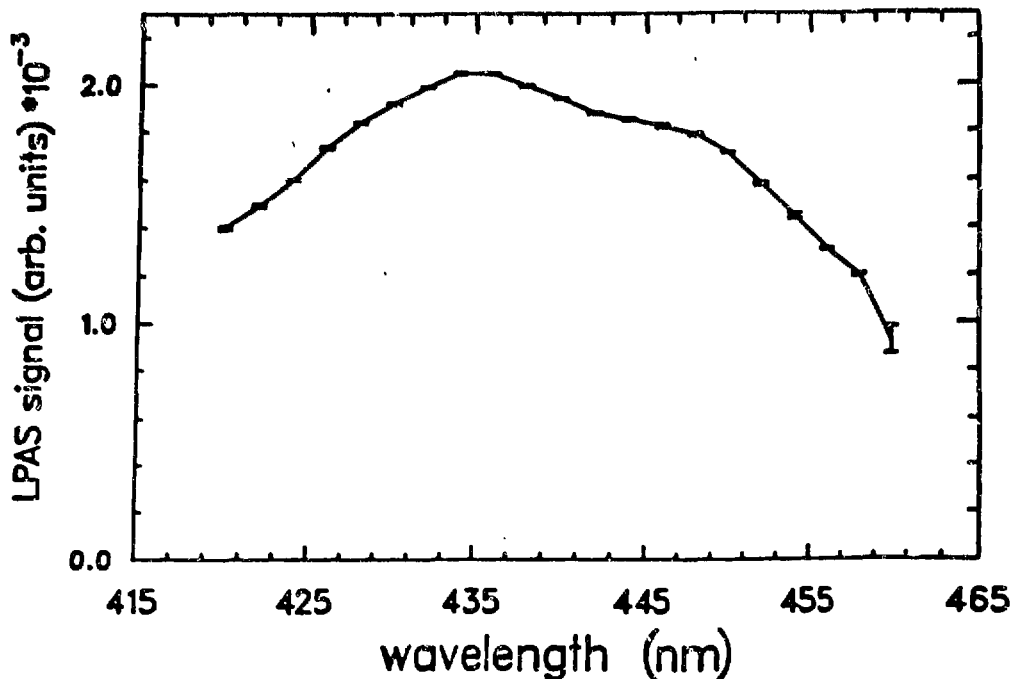


Figure 7. Photoacoustic spectrum observed from  $1.1 \times 10^{-4}$  M uranyl ( $\text{UO}_2^{2+}$ ) in GR-4 water (synthetic basalt groundwater) at  $76^\circ\text{C}$ . Data were recorded every 2 nm. The error limits shown correspond to the 90% confidence range based on five determinations each of the uranyl vs. GR-4 and GR-4 vs. GR-4 runs with all samples in sealed 1 x 1 cm quartz cuvettes. The differential amplifier gain was reduced by a factor of four compared to Figure 6.

require methods to differentiate between actinides absorbed on colloidal particles, colloidal particles whose bulk is actinide hydroxo species, and colloidal particles whose nucleus is an actinide complex.

## CONCLUSIONS

The sensitivity achieved using our single beam, dual channel, laser photoacoustic spectrometer is essentially identical to that reported by Kim and co-workers [4,5] for work at  $22^\circ\text{C}$  ( $\sim 10^{-5}$  a.u. per cm). Minor differences are likely, due to methods used for interpretation of data. The main difficulty encountered in the initial phases of this work was the lack of reproducibility. Subsequent developments which minimize scattered laser light and the presence of suspended particulate matter have largely eliminated this problem. The LPAS system has been tested in single and dual channel modes at  $76^\circ\text{C}$  using uranyl in GR-4 water. In preliminary investigations we have observed an improved sensitivity in aqueous solution at higher temperatures as expected from photoacoustic theory. In the spectral range investigated, the absorption of water is not a significant limiting factor, however, the need for differential measurements increases (e.g., Pu(VI) absorption at 830 nm) where water absorption is significant. Based on the reported absorption spectra of uranyl carbonate complexes [12], the observed photoacoustic spectra do not arise from a simple mixture of di- and tri-carbonato species.

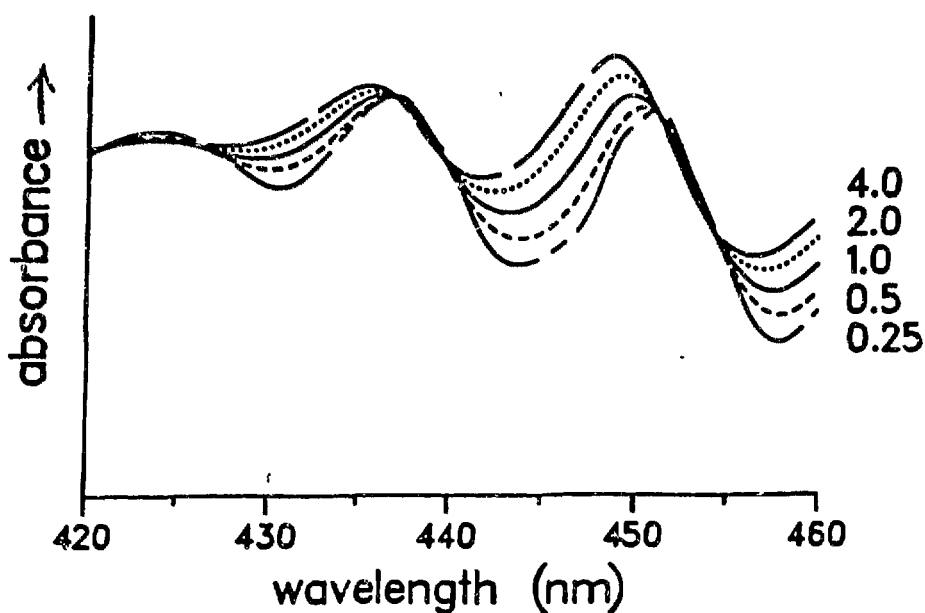


Figure 8. Absorption spectra expected for various ratios of triscarbonato uranyl to dicarbonato uranyl in the 420 nm to 460 nm region.

The high sensitivity of the LPAS technique in aqueous solution at temperature to 100°C and beyond recommends it for actinide speciation studies in basalt groundwater. Future LPAS work will emphasize trans-uranic elements of interest to the BWIP effort in synthetic groundwater solution. This will necessitate acquisition of reference spectra of complexes of these elements in chemically simpler solutions to facilitate speciation. Additional developments of our LPAS system will be directed toward simplifying channel balancing while achieving high rejection of solvent background absorbance. Laser induced fluorescence will be explored as a complementary technique to the LPAS method. The goal of this work is designed to achieve actinide speciation in groundwater under conditions anticipated to exist in the repository after containment failure.

#### ACKNOWLEDGMENTS

Work performed under the auspices of the Office of Basic Energy Sciences, Division of Chemical Sciences, U.S. Department of Energy, under contract number W-31-109-38 and U.S. Department of Energy, Office of Crystalline Repositories, Basalt Waste Isolation Project, under contract number DE-AC06-77RL01030.

#### REFERENCES

1. W. T. Carnall, Handbook on the Physics and Chemistry of the Rare Earths, Vol. 3, K. A. Geschneider and L. Eyring, eds., (North Holland, Amsterdam), 1979, pgs 171-208.
2. W. T. Carnall and H. M. Crosswhite, Optical Spectra and Electronic Structure of the Actinides in Compounds and Solutions, Argonne National Laboratory Report ANL-84-90, August 1985.

3. C. K. N. Patel and A. C. Tam, Review of Modern Physics, 53, 517-550, (1981).
4. W. Schrepp, R. Stumpe, J. I. Kim, and H. Walther, Appl. Phys. B, 32, 207-209 (1983).
5. R. Stumpe, J. I. Kim, W. Schrepp, and H. Walther, Appl. Phys. B, 34, 203-206 (1984).
6. T. W. Newton and J. C. Sullivan, Handbook on the Physics and Chemistry of the Actinides, A. J. Freeman and C. Keller, eds., Elsevier Science, pp. 387-405 (1985).
7. R. Stumpe and J. I. Kim, "Laser-Induzierte Photoakustische Spectroskopie Zum Nachweis Des Chemischen Verhaltnes Von Aktiniden Im Natuerlichen Aquatischen System," RCM 02386 (June 1986).
8. R. J. Lemire and P. R. Tremaine, J. Eng. Data, 25, 361 (1980).
9. J. A. Dill, T. E. Jones, D. Marcy, M. O. Baechler and J. R. Payne, Rep. SD-BWI-TD-013, Hanford Operations Basalt Waste Isolation Project, 12-4-84.
10. IUPAC conformances, Anal. Chem., 58, 269 (1986).
11. J. T. Bell and R. E. Biggers, J. Mol. Spec., 18, 247-275 (1965).
12. J. P. Scanlan, J. Inorg. Nucl. Chem., 39, 625-639 (1977).